Study of the Photodissociation Process of ClC(O)SCH3 Using both Synchrotron Radiation and HeI Photoelectron Spectroscopy in the Valence Region

ARTICLE *in* THE JOURNAL OF PHYSICAL CHEMISTRY A · AUGUST 2010

Impact Factor: 2.69 · DOI: 10.1021/jp102179w · Source: PubMed

6 AUTHORS, INCLUDING:

Mauricio Federico Erben
National University of La Plata
90 PUBLICATIONS **792** CITATIONS
SEE PROFILE

Mao-Fa Ge
Chinese Academy of Sciences
259 PUBLICATIONS **3,004** CITATIONS
SEE PROFILE

Reinaldo Cavasso-Filho
Universidade Federal do ABC (UFABC)
48 PUBLICATIONS **267** CITATIONS
SEE PROFILE

Carlos O. Della Vedova
National University of La Plata
293 PUBLICATIONS **2,673** CITATIONS
SEE PROFILE

Study of the Photodissociation Process of $ClC(O)SCH_3$ Using both Synchrotron Radiation and HeI Photoelectron Spectroscopy in the Valence Region

Mariana Geronés,[†] Mauricio F. Erben,*[,†] Maofa Ge,[§] Reinaldo L. Cavasso Filho,[||] Rosana M. Romano,*[,†] and Carlos O. Della Védova[†,‡]

CEQUINOR (CONICET-UNLP), Departamento de Química, Facultad de Ciencias Exactas, Universidad Nacional de La Plata, C.C. 962 (1900) La Plata, Argentina, Laboratorio de Servicios a la Industria y al Sistema Científico (LaSeISiC), UNLP-CIC-CONICET, Camino Centenario e/505 y 508, (1903) Gonnet, Argentina, State Key Laboratory for Structural Chemistry of Unstable and Stable Species, Beijing National Laboratory for Molecular Sciences (BNLMS), Institute of Chemistry, Chinese Academy of Sciences, Beijing 100080, People's Republic of China, and Universidade Federal do ABC, Rua Catequese, 242, CEP 09090-400, Santo André, São Paulo, Brazil

Received: March 10, 2010; Revised Manuscript Received: June 2, 2010

The simultaneous evaluation of the PES and valence synchrotron photoionization studies complemented by the results of quantum chemical calculations offers unusually detailed insights into the valence ionization processes of small covalent molecules. Thus, methyl thiochloroformate, $ClC(O)SCH_3$, has been investigated by using results from both photoelectron spectroscopy (PES) and synchrotron radiation in the valence energy range. In an additional series of experiments, total ion yield (TIY) and photoelectron−photoion coincidence (PEPICO) spectra have been recorded. Furthermore, the relative yields for ionic fragments have been determined as a function of the photon energy. Vibronic structure has been observed in the TIY spectrum recorded in the synchrotron experiments. The photodissociation behavior of $ClC(O)SCH_3$ can be divided into two well-defined energy regions.

Introduction

Photoionization studies concerning the sulfenylcarbonyl −C(O)S− compounds FC(O)SCl,[1,2] ClC(O)SCl,[3] $CH_3C(O)SH$,[4] and $CH_3OC(O)SCl$[5] have been recently reported by our group. By using synchrotron radiation in the range 100−1000 eV, total ion yield (TIY) and partial ion yield (PIY) spectra as well as time-of-flight (TOF) multicoincidence spectra [photoelectron−photoion coincidence (PEPICO) and photoelectron−photoion−photoion coincidence (PEPIPICO)] have been measured around the main ionization edges.

The recent development of a neon gas filter in the TGM line at the Brazilian Synchrotron National Laboratory (LNLS) which affords "pure" synchrotron radiation in the 12−21.5 eV range has allowed us to expand the study on electronic properties and photoionization dynamics into the valence region. Thus, sulfenylcarbonyl compounds such as FC(O)SCl,[6] ClC(O)SCl,[6] and $CH_3C(O)SCH_3$[7] have been recently analyzed by using the combination of photoelectron spectroscopy (PES) and results derived from the use of synchrotron radiation in the same energy range. The simultaneous evaluation of the results from both photoelectron spectroscopy (PES) and synchrotron photoionization measurements, complemented by high level ab initio calculations, provides unusually detailed insights into the valence ionization processes of these molecules. For instance, in the case of $CH_3C(O)SCH_3$, five of the resonant (optical) transitions in the TIY spectrum display vibronic structure.[7]

In the present work, we report a study of the photon impact excitation and ionization dissociation dynamics on another member of the carbonylsulfenyl family, namely methyl thiochloroformate ($ClC(O)SCH_3$). The methodology includes the use of synchrotron-based multicoincidence TOF mass spectroscopic techniques together with the acquisition of the "typical" photoelectron spectra using the HeI line as photon source. The total ion yield spectrum together with the PEPICO spectra at selected photon energies using synchrotron radiation in the valence region has been measured, thereby allowing the study of the dissociation dynamics of excited $ClC(O)SCH_3$ molecules.

Relevant studies have been reported for the title molecule. Thus, its molecular structure and conformational behavior have been investigated in both the gas and crystalline states by means of infrared studies of the matrix-isolated molecules and X-ray crystallographic analysis of single crystals at low temperatures.[8] Hence the predominance of the syn rotamer in the vapor has been confirmed (i.e., C═O double bond in synperiplanar orientation with respect to the $S-CH_3$ single bond) and the crystal of the compound is composed exclusively of the planar syn rotamer, with overall C_s symmetry. Previous studies of the microwave spectrum,[9] vibrational spectrum,[10] and gas electron diffraction pattern[11] agree with the fact that $ClC(O)SCH_3$ has a planar structure with syn conformation in the vapor. Furthermore, the photochemistry of $ClC(O)SCH_3$ isolated in solid Ar or N_2 matrixes at 15 K has been investigated.[12] On the basis of the evidence of the matrix IR spectra its irradiation photoproducts were identified using broad-band UV−visible light. Thus, in the first place both CO and $ClSCH_3$ are formed, and in a subsequent step, a hydrogen atom is detached from the methyl group forming an $H_2C{=}S\cdots HCl$ molecular complex.

Experimental Section

Synchrotron radiation from the Brazilian Synchrotron Light Source (LNLS) was used. Linearly polarized light monochromatized by a toroidal grating monochromator (available at the

[†] Universidad Nacional de La Plata.
[‡] UNLP-CIC-CONICET.
[§] Chinese Academy of Sciences.
[||] Universidade Federal do ABC.

10.1021/jp102179w
Published on Web 07/21/2010

TGM beamline in the range 12−310 eV)[13] intersects the effusive gaseous sample inside a high-vacuum chamber at a base pressure in the range of 10^{-8} mbar. During the experiments, the pressure was maintained below 2×10^{-6} mbar. The intensity of the emergent beam was recorded by a light-sensitive diode. The photon energy resolution from 12 to 21.5 eV was given by $E/\Delta E = 550$. The ions produced by the interaction of the gaseous sample with the light beam were detected by means of a time-of-flight (TOF) mass spectrometer of the Wiley−McLaren type for PEPICO measurements. This instrument was constructed at the Institute of Physics, Brasilia University, Brasilia, Brazil.[14] The axis of the TOF spectrometer is perpendicular to the photon beam and parallel to the plane of the storage ring. Electrons are accelerated to a multichannel plate (MCP) and recorded without energy analysis. This event starts the flight time determination process for the corresponding ion, which is consequently accelerated to another MCP. High-purity vacuum-ultraviolet photons are used; the problem of contamination by high-order harmonics can be suppressed by the innovative gas-phase harmonic filter recently installed at the TGM beamline at the LNLS.[15−17]

The HeI PE spectrum of $ClC(O)SCH_3$ was recorded on a double-chamber UPS-II machine built specifically to detect transient species at a resolution of about 30 meV, as indicated by the $Ar^+(^2P_{3/2})$ photoelectron band.[18−24] Experimental vertical ionization energies (I_v in electronvolts) were calibrated by simultaneous addition of small amounts of argon and iodomethane to the sample.

OVGF calculations[25] using the 6-311++G(d,p) basis set and B3LYP/6-311++G(d,p)-optimized geometry of the syn conformer have been performed on $ClC(O)SCH_3$ in its ground electronic state using the Gaussian 03 program package.[26] The energies of dissociation of the $ClC(O)SCH_3^{\bullet+}$ parent radical ion into possible fragments were calculated at the UB3LYP/6-311++G (d,p) level of approximation.

The sample of $ClC(O)SCH_3$ was obtained from a commercial source (Aldrich, estimated purity better than 95%). The liquid was purified by repeated trap-to-trap condensations at reduced pressure in order to eliminate volatile impurities. The final purity of the compound in both the vapor and the liquid phases was carefully checked by IR and Raman spectroscopies.[8,12]

Results and Discussion

It is well-established that the molecule of $ClC(O)SCH_3$ in its electronic ground state belongs to the C_s symmetry point group. It follows that all the canonical molecular orbitals of type a′ are σ-orbitals lying in the molecular plane, while those of type a″ are π-orbitals. The 30 valence electrons are then arranged in 15 double-occupied orbitals in the independent particle description.

Photoelectron Spectra. The HeI PE spectrum of $ClC(O)SCH_3$ is depicted in Figure 1, and the experimental and theoretical vertical ionization energies are listed in Table 1. Assignments were made with reference to the results of the OVGF/6-311++G(d,p) calculations (optimized geometry for the syn conformer at the B3LYP/6-311++G(d,p) level of approximation).

A comparison with the PES previously reported for similar species gives confidence to the proposed band assignment.[6,7,27,28] The characters of the 12 highest occupied molecular orbitals of $ClC(O)SCH_3$ are shown in Figure 2.

The first ionization band appearing in the spectrum at 10.11 eV can be assigned to the ionization process from the HOMO, an n″(S) orbital, which can be visualized as a lone pair

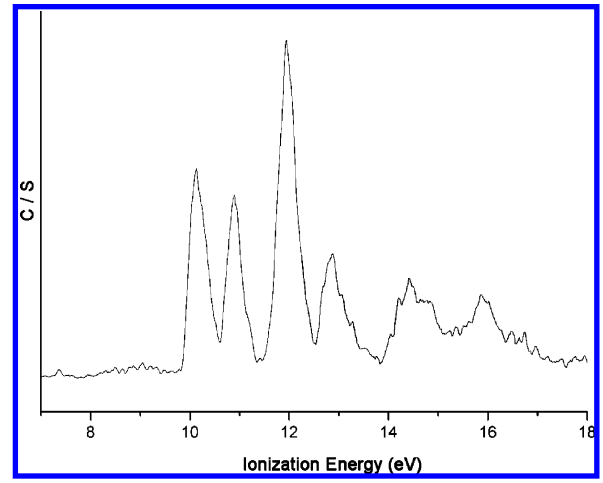

Figure 1. HeI photoelectron spectrum of $ClC(O)SCH_3$.

TABLE 1: Experimental and Calculated Ionization Energies and MO Characters for $ClC(O)SCH_3$

PES (eV)	calcd[a] (eV)	MO	character	TIY (eV)	VS[b] (cm^{-1})
10.11	9.88	28	n″(S)	−	
10.88	10.90	27	n′(O)	−	
11.96	11.58	26	n″(Cl)	12.07	
	11.68	25	n′(Cl)		
12.88	12.78	24	$\pi''_{C=O}$	13.14	
14.44	14.84	23		13.75	
14.82	15.00	22	$\sigma_{C-H}(CH_3)$	14.25	
15.85	15.79	21		16.06	1288 ± 40
	16.42	20	$\sigma_{S-C}(SCH_3)$	16.33	
	16.57	19	n′(S)	16.93	
	18.64	18	$\sigma_{Cl-C}(C=O)$		
		17	$\sigma_{S-C}(C=O)$		

[a] Calculated values at the OVGF/6-311++G(d,p) level of approximation with B3LYP/6-311++G** optimized geometries. [b] VS indicates band with vibronic structure observed in the TIY spectrum.

nominally localized at the sulfur atom. The second ionization potential, observed at 10.88 eV, is assigned to the ionization processes of an electron ejected from another predominantly nonbonding orbital, the n′(O) orbital. The following band in the PES of $ClC(O)SCH_3$ at 11.96 eV is associated with the ionization process involving both the a″ and a′ nonbonding orbitals of the chlorine atom. It should be noted that OVGF calculations reproduce this observation, with similar ionization potential (IP) values (11.58 and 11.68 eV) for n″(Cl) and n′(Cl) orbitals. The 12.88 eV band in the PES is related to the ionization from the π-orbital in the carbonyl double bond.

A diagrammatic representation of the experimentally determined IPs for molecular orbitals formally located at the sulfenylcarbonyl group for a series of simple −SC(O)− containing species is shown in Figure 3. Taking $ClC(O)SCH_3$ as reference, it is observed that the substitution of the chlorine atom by electron-releasing alkyl groups causes a reduction of the IP values. Thus, the three orbitals shown in Figure 3 are less stabilized in the $CH_3C(O)SCH_3$[7] molecule compared with the other species. On the other hand, substitution of the chlorine atom by more electronegative groups leads to higher IP values. Thus, FC(O)SCl shows the highest ionization potential value. It should be remarked that FC(O)SCl is isoelectronic with the title species and, thus, electronic correlation effects should have similar importance in both species.

The trend observed in Figure 3 shows a clear dependence on the substituents attached to the sulfur atom. Thus, in the series

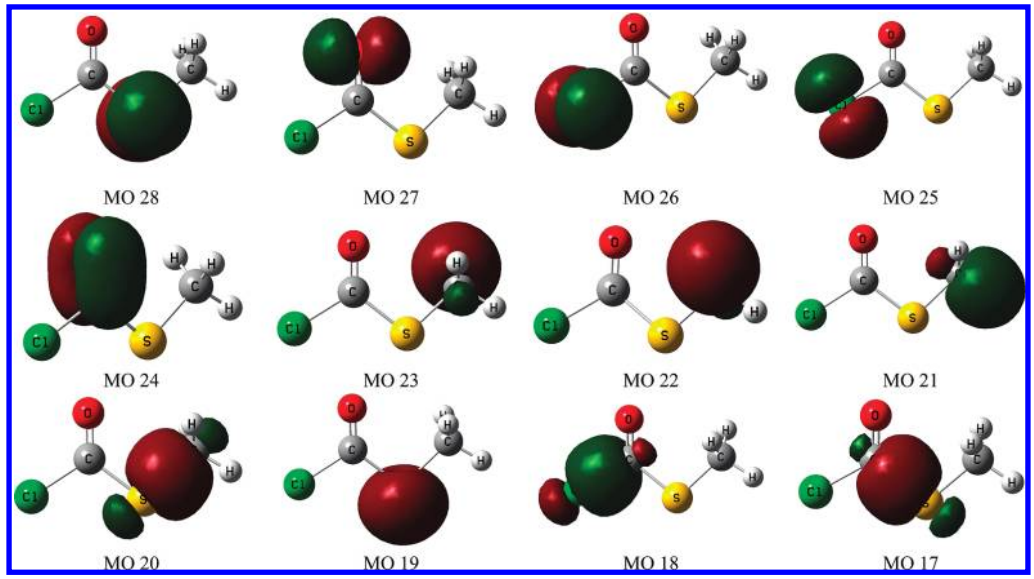

Figure 2. Schematic representation of the 12 highest occupied molecular orbitals of $ClC(O)SCH_3$ calculated at the UB3LYP/6-311++G(d,p) approximation.

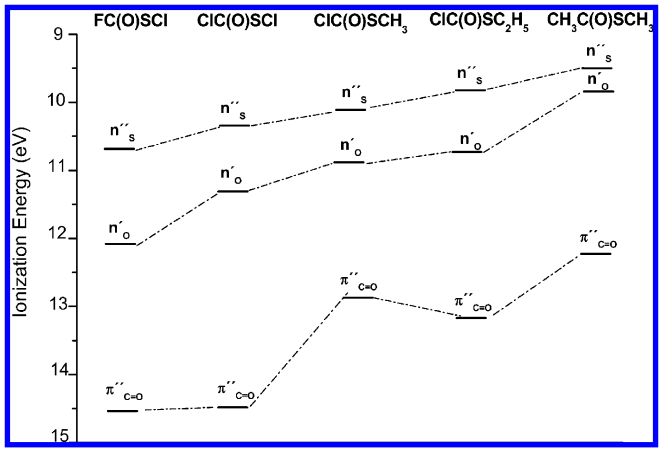

Figure 3. Correlation diagram of the ionization potentials of −SC(O)− containing compounds.[6,7]

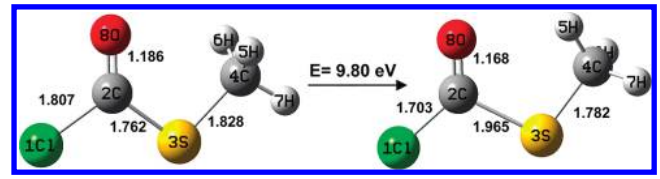

Figure 4. Molecular models of $ClC(O)SCH_3$ in its neutral ground state (left) and singly charged low-lying cationic state (right), showing selected bond distances and adiabatic ionization energy calculated at the UB3LYP/6-311++G(d,p) level of approximation.

of $ClC(O)SX$ (X = CH_3, Cl, and C_2H_5) species, the ClC(O)SCl molecule possesses higher stabilization of the n″(S), n′(O), and $\pi''_{C=O}$ orbitals.

When a chlorine atom is formally substituted by either the CH_3 or CH_2CH_3 group, the ionization energy associated with molecular orbitals of the −SC(O)− moiety is definitively lower, denoting the electron-releasing properties of the alkyl groups. Moreover, the highest stabilization of the $\pi''_{C=O}$ orbitals observed in this series for both ClC(O)SCl and FC(O)SCl could be associated with the importance of the π-electronic conjugation (resonance interactions) forming a delocalized and extended π-system favored by the planarity of these molecules.

Calculations (UB3LYP/6-311++G(d,p)) were performed to analyze the nature of the low-lying cationic radical formed in the first ionization process. As is evident from the details set out in Table 2, the atomic charges are delocalized over the −C(O)S− group, probably favored by the planarity of both the neutral and ionized forms (see below). An appreciable fraction of positive charge is localized at the S atom, which increases 0.503 unit upon ionization (see also the characters of the first ionization process of Table 1 and of MO 28 in Figure 2).

The heavy-atom planar skeleton of the $ClC(O)SCH_3$ molecule remains unchanged after simple ionization with a remarkable elongation of about 0.23 Å of the C2−S3 single bond and the shortening of the other bonds lengths (Figure 4). The syn orientation of the C═O and S−C bonds is retained after ionization. The calculated value of the adiabatic IP is 9.80 eV at the UB3LYP/6-311++G(d,p) approximation.

Photoionization Processes. For absorptions above the ionization thresholds, the quantum yield for molecular ionization is quite likely to tend to unity; i.e., for each photon absorbed, an ion is produced. Consequently, the detection of parent and fragment ions as a function of the incident photon energy (TIY) is a powerful method that complements absorption spectroscopy.[29] Thus, an increment in the total ion production is expected

TABLE 2: Atomic Charges for the Molecular and Cation-Radical Forms of $ClC(O)SCH_3$ Calculated with the UB3LYP/6-311++G(d,p) Approximation[a]

	atom								
	Cl_1	C_2	S_3	C_4	H_5	H_6	H_7	O_8	TAC[b]
$ClC(O)SCH_3$	0.329	−0.450	0.262	−0.548	0.176	0.176	0.156	−0.103	0
$ClC(O)SCH_3^+$	0.600	−0.500	0.765	−0.661	0.254	0.260	0.243	0.039	+1
Δq[c]	0.271	−0.050	0.503	−0.215	0.078	0.084	0.087	0.142	+1

[a] For atom numbering, see Figure 4. [b] Total atomic charge. [c] $\Delta q = q(ClC(O)SCH_3^+) - q(ClC(O)SCH_3)$.

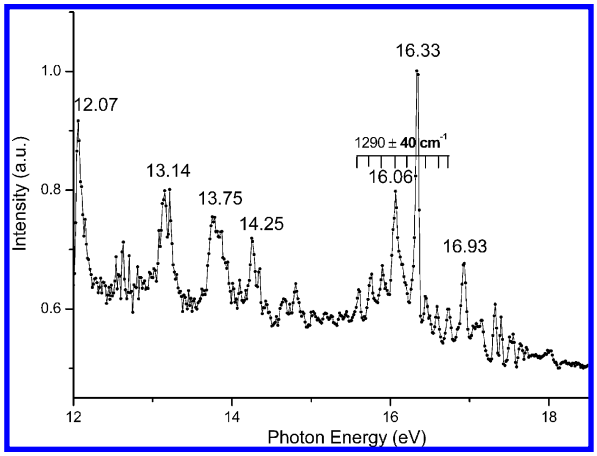

Figure 5. TIY spectrum of $ClC(O)SCH_3$ in the photon energy range 12.0−18.5 eV.

every time that the incident energy exceeds a particular ionization potential as defined in PES conditions; the magnitude of the increment depends on the cross section of the particular ionic state. As is well-known, however, a valence ionic state—even one outside the ground state's Franck−Condon region—can be resonantly populated using tunable synchrotron radiation throughout a transition from the ground electronic state to a neutral Rydberg state, followed by a subsequent autoionization process. Similar, but not identical, transition energies are therefore expected when PES and TIY spectra are compared.

The TIY spectrum of $ClC(O)SCH_3$ in the photon energy range 12.0−18.5 eV is depicted in Figure 5. Comparison between the PES and TIY spectra is feasible for the outermost ionization states, for which the photoelectron spectrum shows clearly defined bands. The PES is poorly resolved at ionization energies above approximately 14.0 eV, which are usual for many processes in organic species. Thus, in the low energy ionization region (E < 14.5 eV) there are a group of well-defined signal bands in the TIY spectrum with no obvious vibrational structure. The maximum of the first band observed in the TIY spectrum occurs at 12.07 eV and correlates with the band near 11.96 eV in the PES of $ClC(O)SCH_3$, assigned to the ionization of electrons formally located at nonbonded orbitals of the chlorine atom.

The 13.14 eV transition observed in the TIY spectrum is assigned to the ionization related to a transition from the $\pi_{C=O}$ orbital in a similar way to its counterpart in the PES spectrum at 12.88 eV. The next three bands centered at 13.75, 14.25, and 16.06 eV are assigned to ionizations involving the σ_{C-H} orbital of the CH_3 group bonded to the sulfur atom. The last of these bands displays vibronic structure with a progression of $\nu_o = 1290 \pm 40$ cm^{-1}. Tentatively, this progression can be identified with a vibrational fundamental in which the deformation of the methyl group is the dominant motion. The $\delta(CH_3)$ normal modes of vibration of the matrix-isolated neutral $ClC(O)SCH_3$ molecule occur at 1433.6, 1420.0, and 1320.4 cm^{-1} for the two antisymmetrical and symmetrical representations, respectively.[12] A very similar vibrational progression is observed in the TIY spectrum of $CH_3C(O)SCH_3$, where the 15.66 eV band associated with the excitation of electrons of the methyl group displays a vibrational structure with $\nu_o = 1288 \pm 40$ cm^{-1}.[7]

The remaining transitions, at 16.33 and 16.93 eV, in the TIY spectrum can be associated with processes involving the $\sigma_{S-C}(SCH_3)$ and n′(S) orbitals, respectively.

PEPICO spectra of $ClC(O)SCH_3$ were measured at different photon energies corresponding to each maximum of the TIY spectrum depicted in Figure 5, and also at some off-resonance energy values. The relative intensities for the main fragment ions as a function of the photon energy are summarized in Table 3. The intensity of each ionic fragment is obtained as the integrated area under the corresponding peak, by fitting a Gaussian function to the TOF spectra. Naturally occurring isotopomer fragments, mainly due to the presence of ^{35}Cl and ^{37}Cl isotopes, are clearly observed due to the suitable mass resolution attained in the experiments. This fact assists the assignment of the ion fragments appearing in the coincidence spectra.

The lowest energy delivered by the TGM beamline at the LNLS (12.00 eV) is higher than the first ionization potential of the $ClC(O)SCH_3$ molecule (10.11 eV). Therefore, ionization processes from MO 28 and MO 27 (Table 1) can already be observed at this very first stage of the experiment. A detailed analysis of the PEPICO spectra shows remarkable differences in the relative abundances of the ions produced as a function of the energy of the incident photons, revealing that the title molecule possesses a very rich photofragmentation dynamics. For the description of the different fragmentation patterns observed in the PEPICO spectra, we will group the ones that present similar behaviors.

The PEPICO spectrum obtained at 12.63 eV (Figure 6), an energy that may be considered as far from resonances, is dominated by a signal corresponding to $C(O)SCH_3^+$ (75 amu/q), followed in relative abundance by the molecular ion (110 and 112 amu/q) and OCS^+ (60 amu/q). The HCl^+ (36 and 38 amu/q), H_2Cl^+ (37 and 39 amu/q), and CH_3CO^+ (43 amu/q) species are also discernible in this spectrum.

In the PEPICO spectrum obtained with 12.07 eV photons (Figure 6), the only one taken with an energy below 12.63 eV, $C(O)SCH_3^+$ remains as the most intense fragment but the relative intensity of OCS^+ is notably increased with respect to the former spectrum. The parent cation is also observed, in this case in third place. The incident energy coincides with a maximum in the TIY spectra of Figure 5, assigned to the ionization of electrons formally located at nonbonded orbitals of the chlorine atom.

The 14 spectra taken at photon energies between 13.14 and 15.36 eV (some of them are shown in Figure 6) can be analyzed together. In all of them the spectra the general pattern observed in the 12.36 eV spectrum is maintained, increasing the number of ions and their relative abundances as the photon energy increases. Besides the fragments already described, SCH_3^+ (47 amu/q), $ClCO^+$ (63 and 65 amu/q), and SCH_2^+ (46 amu/q), in order of relative intensities, appear from the 13.14 eV spectrum. The 13.75 eV incident energy opens the fragmentation channels to lighter species such as CS^+ (43 amu/q), CH_3^+ (15 amu/q), and S^+ (32 amu/q). Access to the ionization channel for the production of CO^+ (28 amu/q) is gained from 13.87 eV, while HCS^+ (45 amu/q) becomes discernible from 14.25 eV.

When the sample is irradiated with photons of 15.45 (see Figure 7), 15.60, and 15.76 eV, the OCS^+ signal dominates the spectra. At 16.44 and 16.59 eV both S^+ and OCS^+ are the most abundant fragments. Notoriously, the HCl^+ species is the most intense feature in the PEPICO spectrum measured at 15.90 eV (Figure 7) (it should noted that the relative abundances in Table 3 refer only to $H^{35}Cl^+$).

The PEPICO spectra taken at 16.06, 16.33 (Figure 7), 16.93, and 17.32 eV are very similar, with all of them dominated by a very intense signal of CS^+, followed by $C(O)SCH_3^+$ and HCl^+ as the most abundant of the remaining fragments. The other spectra measured with energies higher than 15.36 eV (at 15.94,

TABLE 3: Relative Intensities (PIY %) Photoionization Yield (%) for the Main Fragment Ions Extracted from PEPICO Spectra as a Function of Photon Energy for $ClC(O)SCH_3$

	branching ratios at various *m/z* values (amu/*q*)													
photon energy (eV)	15 CH_3^+	28 CO^+	32 S^+	36[a] HCl^+	37[a] H_2Cl^+	43 CH_3CO^+	44 CS^+	45 HCS^+	46 SCH_2^+	47 SCH_3^+	60 OCS^+	63 $ClCO^+$	75 $COSCH_3^+$	110[a] $ClC(O)SCH_3^+$
12.07	–	–	–	–	–		–	–	–	–	33.0	–	42.0	13.0
12.63	–	–	–	1.8	0.7	0.8	–	–	–	–	8.1	0.8	63.0	14.0
13.14	–	–	–	1.1	0.5	1.0	–	–	0.3	3.3	24.0	0.8	50.0	9.1
13.21	–	–	–	1.1	0.6	0.9	–	–	0.3	4.0	18.0	0.9	56.0	10.0
13.75	0.9	–	0.8	1.4	0.7	1.0	1.8	–	0.3	7.4	19.0	1.0	47.0	8.2
13.83	0.9	–	0.8	1.0	0.6	1.1	1.7	–	0.4	8.2	18.0	1.0	49.0	8.4
13.87	1.1	2.0	0.6	1.2	0.7	1.2	1.7	–	0.4	8.5	15.0	1.0	50.0	8.3
14.11	2.3	2.0	0.6	1.4	0.6	1.3	1.3	–	0.5	11.0	7.5	1.0	53.0	8.6
14.25	2.7	1.6	1.2	1.5	0.7	1.5	0.9	0.6	0.8	10.0	15.0	1.0	43.0	7.5
14.35	3.4	1.2	0.8	1.9	0.8	1.3	0.8	0.7	0.9	12.0	10.0	1.0	48.0	8.0
14.65	5.0	1.5	1.1	1.8	1.1	1.5	0.7	1.5	1.1	13.0	9.4	2.0	42.0	7.6
14.85	5.7	1.6	1.1	1.6	1.1	1.5	0.8	2.4	1.3	13.0	8.5	2.0	41.0	7.5
14.89	6.1	1.3	1.0	1.6	1.0	1.5	0.7	2.6	1.3	13.0	7.2	2.0	42.0	7.7
15.18	5.6	1.4	3.4	3.6	1.6	1.9	1.6	3.2	1.2	12.0	14.0	2.0	34.0	6.2
15.27	6.6	2.2	3.2	2.8	1.8	2.4	1.6	3.8	2.0	11.0	10.0	2.0	31.0	7.0
15.36	6.6	2.5	4.0	3.3	2.0	2.5	1.8	4.0	2.1	10.0	9.2	2.0	29.0	6.9
15.45	2.7	2.2	9.8	9.3	4.3	2.8	6.5	1.9	1.2	4.8	29.0	1.0	11.0	2.4
15.60	3.2	2.0	8.9	10.0	5.1	3.1	11.0	2.4	1.4	5.2	19.0	1.0	12.0	2.7
15.76	3.5	2.3	9.0	10.0	4.1	3.3	13.0	2.8	1.5	5.5	16.0	1.0	12.0	3.0
15.90	3.9	2.1	8.4	12.0	4.0	3.5	15.0	3.2	1.7	5.8	11.0	1.0	13.0	3.2
15.94	7.8	2.0	4.8	2.6	1.6	2.3	2.2	6.3	2.4	12.0	5.8	2.0	29.0	6.8
16.06	4.5	2.1	4.0	7.1	3.5	3.8	26.0	3.9	2.2	5.9	4.9	2.0	12.0	4.0
16.33	4.9	2.8	3.4	4.4	2.9	3.9	27.0	4.0	2.7	5.3	4.1	2.0	10.0	4.7
16.44	3.3	3.9	16.0	10.0	4.2	3.0	9.7	3.0	1.5	5.2	16.0	1.0	10.0	2.4
16.50	8.4	2.1	4.6	2.4	1.6	2.3	1.6	7.8	2.8	12.0	5.0	2.0	28.0	6.7
16.59	3.2	4.5	18.0	9.2	4.1	2.9	8.0	2.9	1.5	5.1	17.0	1.0	9.9	2.3
16.72	7.3	2.2	7.4	3.9	2.0	2.0	3.7	7.8	2.1	12.0	7.1	3.0	25.0	5.5
16.93	4.7	2.7	5.2	7.7	3.1	2.1	22.0	3.3	1.9	6.3	5.4	2.0	12.0	3.8
17.08	8.3	2.6	4.5	2.5	1.7	2.3	1.9	8.6	2.9	12.0	4.7	2.0	26.0	6.6
17.16	7.5	2.7	7.7	3.6	1.9	1.9	3.3	8.4	2.2	12.0	7.1	3.0	25.0	5.5
17.32	4.8	2.4	5.9	8.3	4.2	3.9	20.0	4.6	2.4	6.4	6.0	2.0	12.0	3.9
17.50	8.0	2.9	5.3	2.8	1.7	2.8	2.6	8.1	3.0	11.0	5.4	2.0	23.0	6.5
17.55	7.0	3.9	6.4	4.1	2.1	3.4	4.5	6.5	3.0	8.4	6.5	2.0	17.0	6.1
17.64	7.2	3.9	6.2	3.9	2.0	3.5	3.6	6.7	3.1	8.6	6.4	2.0	18.0	6.2
17.71	7.3	3.7	6.1	3.6	2.0	3.4	3.3	6.9	3.2	8.9	6.2	2.0	18.0	6.2

[a] Peaks for the corresponding naturally occurring isotopomer were observed.

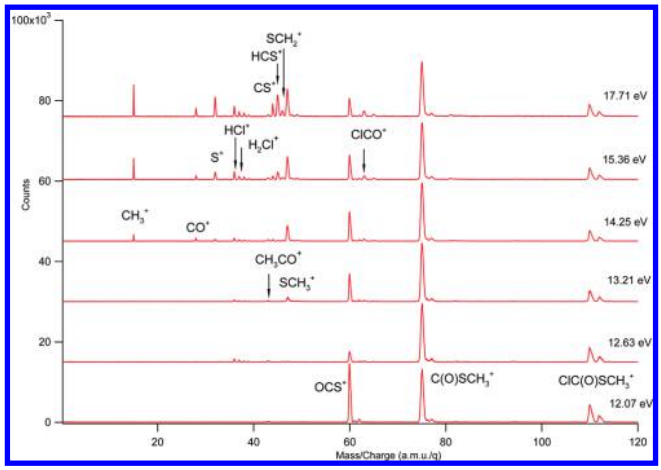

Figure 6. PEPICO spectra of $ClC(O)SCH_3$ taken at selected energies: 12.07, 12.63, 13.21, 14.25, 15.36, and 17.71 eV.

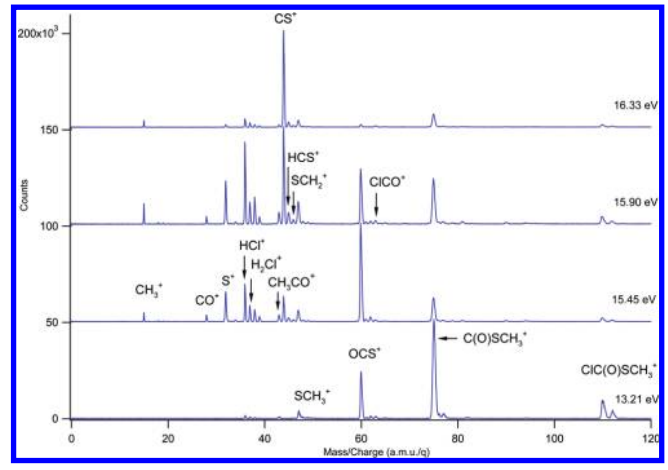

Figure 7. PEPICO spectra of $ClC(O)SCH_3$ taken at selected energies: 13.21, 15.45, 15.90, and 16.33 eV.

16.50, 16.72, 17.08, 17.16, 17.50, 17.55, 17.64, and 17.71 (Figure 6) eV) do not differ significantly from the ones between 13.14 and 15.36 eV described above.

The previous description reveals the complexity of the energy dependence of the fragmentation dynamics after photoionization of $ClC(O)SCH_3$. Several fragmentation channels, which seem to alternate with the energy of the incident radiation, are feasible for this molecule.

It is worth noting that the relative intensities in the PEPICO spectra between HCl^+ and H_2Cl^+, two species that are formed after a molecular rearrangement, do not vary significantly along the whole energy range studied. Moreover, HCl^+ appears with an abundance greater than 1% in all the measured spectra (with the exception of the spectrum taken at 12.07 eV), being the most abundant ion detected with 15.9 eV ionizating radiation. These two observations suggest that the formation of HCl^+ after

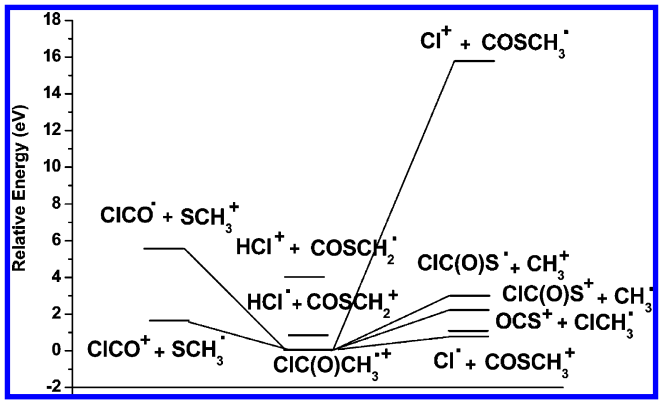

Figure 8. Energy profiles for dissociation of the molecular ion $ClC(O)SCH_3^+$.

phoionization of $ClC(O)SCH_3$ is a favored process and also that the mechanisms of the formation of H_2Cl^+ may be in some way related with the production of HCl^+. These observations coincide with a recent prediction of Neufeld and Wolfire[30] that based on thermochemical considerations HCl^+ and H_2Cl^+ are potentially detectable in interstellar photodissociation regions. In the proposed mechanisms the Cl^+ ion captures an H atom to form HCl^+, which subsequently produces another H abstraction reaction, giving H_2Cl^+.

It is also important to notice the contribution of the HCS^+ ion to the spectra, particularly at high energies (see Table 3). This ion has been observed in the ionic fragmentation of other sulfur compounds having a methyl group.[31] The high thermodynamic stability of this interstellar species as been already pointed out.[32]

Flammang, Nguyen, and collaborators have studied the unimolecular chemistry of a series of *S*-alkyl thioformate, $HC(O)SR^{\bullet+}$, radical cations.[33,34] Decarbonylation of the molecular ions is a common process, and the $[M - 28]$ ion is readily observed by using tandem mass spectrometry methodologies. For $HC(O)SCH_3$, the proposed mechanism consists of a 1,2-hydrogen shift giving rise to the formation of a sulfurane intermediate ion.[35] However, the $[M - 28]^+$ ion is absent in the photon-excited PEPICO spectra of $ClC(O)SCH_3$ over the whole range of photon energies analyzed here. The CO extrusion is observed in the UV photolysis of matrix-isolated $ClC(O)SCH_3$, where CO and $ClSCH_3$ are the main products observed by infrared spectroscopy.[12]

At this point it becomes interesting to compare the photon-excited dissociation of the related species $ClC(O)SCH_3$ and $CH_3C(O)SCH_3$. Indeed, strong differences are observed in the PEPICO spectra. For instance, whereas the $COSCH_3^+$ ion is predominantly formed from the title species, it is completely absent in the PEPICO spectra of $CH_3C(O)SCH_3$. On the other hand, the CO^+ ion dominates the spectra of the methylated species, with only a minimal presence of $ClC(O)SCH_3^+$. These major differences denote that the group bonded to the carbon atom of the carbonyl group has a definite role in the electronic properties of this class of compounds.

Quantum chemical calculations were performed to estimate the energies of different pathways for the ionic dissociation of the parent ion. A schematic representation is given in Figure 8. For the rupture of the C−S bond involving the carbonyl carbon atom, quantum chemical calculations predict the $ClCO^+ + {}^{\bullet}SCH_3$ channel favored against the $ClCO^{\bullet} + SCH_3^+$. This is in qualitative agreement with the behavior observed in the PEPICO spectra, where $ClCO^+$ appears at 12.63 eV, whereas photons at energies above 13.14 eV are needed to form the SCH_3^+ ion.

At the very first energy recorded at 12.07 eV (Figure 6), $COSCH_3^+$ is already observed in the PEPICO spectrum and represents the most intense ion signal. This fragment is formed in the energetically most favored Cl−C bond rupture from $ClC(O)SCH_3^{\bullet+}$. The same bond rupture but leading to the formation of Cl^+ is energetically definitively less favored differing by approximately 13 eV from that yielding $C(O)SCH_3^+$. As mentioned before, an important contribution of the OCS^+ ion is observed in the photodissociation of valence excited $ClC(O)SCH_3$ at 12.07 eV and can be related to the fact that the dissociation pathway leading to the formation of this ion ($OCS^+ + ClCH_3$) is energetically favored. The dissociation channel leading to the formation of HCl^+, possibly by a rearrangement process from the parent ion, is expected to be present in the photodissociation of valence excited $ClC(O)SCH_3$.

Conclusions

HeI photoelectron spectroscopy (PES) and valence photoionization studies using synchrotron radiation, complemented by density functional theory calculations, have been used in the same energy range to investigate the behavior of $ClC(O)SCH_3$.

The transition observed at 16.06 eV in the TIY spectrum displays a vibronic structure with $\nu_o = 1290 \pm 40$ cm^{-1}. The electronic transition and the vibration can be linked with a transition from σ_{C-H} orbitals and with the CH_3 deformation mode of the cationic state, respectively.

The relative abundances of the photodissociation products of $ClC(O)SCH_3$ strongly depend on the excitation radiation in the energy range investigated. For several ionization energies, including off-resonance values, the $COSCH_3^+$ signal appears as the most intense in the spectra. Another group of spectra, excited with photon energies corresponding to the most prominent maxima of the TIY spectrum, are dominated by the CS^+ fragment. OCS^+ is the most abundant positive ion when the sample is irradiated between 15.45, 15.60, and 15.76 eV, and S^+ is the most abundant positive ion at 16.44 and 16.59 eV. A very remarkable result is found with photons of 15.90 eV, for which the most intense signal corresponds to HCl^+.

The dependence of different dissociation channels on the incident radiation can be estimated qualitatively by analyzing the calculated relative stability of the possible ionic and neutral fragments. The simultaneous evaluation of the PES and valence synchrotron photoionization studies represents a valuable tool to clarify the molecular ionization processes.

Acknowledgment. This work has been largely supported by the Brazilian Synchrotron Light Source (LNLS). The authors wish to thank Arnaldo Naves de Brito and his research group for fruitful discussions and generous collaboration during their several stays in Campinas and the TGM and SGM beamline staffs for their assistance throughout the experiments. They also are indebt to the Agencia Nacional de Promoción Científica y Tecnológica (ANPCyT), Consejo Nacional de Investigaciones Científicas y Técnicas (CONICET), and the Comisión de Investigaciones Científicas de la Provincia de Buenos Aires (CIC), República Argentina, for financial support. They also thank the Facultad de Ciencias Exactas, Universidad Nacional de La Plata, República Argentina for financial support. CODV especially acknowledges the DAAD, which generously sponsors the DAAD Regional Program of Chemistry for the República Argentina supporting Latin-American students to make their PhD in La Plata.

References and Notes

(1) Erben, M. F.; Romano, R. M.; Della Védova, C. O. *J. Phys. Chem. A* **2004**, *108*, 3938.

(2) Geronés, M.; Erben, M. F.; Romano, R. M.; Della Védova, C. O. *J. Electron Spectrosc. Relat. Phenom.* **2007**, *155*, 64.

(3) Erben, M. F.; Romano, R. M.; Della Védova, C. O. *J. Phys. Chem. A* **2005**, *109*, 304.

(4) Erben, M. F.; Geronés, M.; Romano, R. M.; Della Védova, C. O. *J. Phys. Chem. A* **2006**, *110*, 875.

(5) Erben, M. F.; Geronés, M.; Romano, R. M.; Della Védova, C. O. *J. Phys. Chem. A* **2007**, *111*, 8062.

(6) Geronés, M.; Erben, M. F.; Romano, R. M.; Della Védova, C. O.; Yao, L.; Ge, M. *J. Phys. Chem. A* **2008**, *112*, 2228.

(7) Geronés, M.; Downs, A. J.; Erben, M. F.; Ge, M.; Romano, R. M.; Yao, L.; Della Védova, C. O. *J. Phys. Chem. A* **2008**, *112*, 5947.

(8) Romano, R. M.; Della Védova, C. O.; Downs, A. J.; Parsons, S.; Smith, C. *New J. Chem.* **2003**, *27*, 514.

(9) Caminati, W.; Bohn, R. K.; True, N. S. *J. Mol. Spectrosc.* **1980**, *84*, 355.

(10) Nyquist, R. A. *J. Mol. Struct.* **1967−1968**, *1*, 1.

(11) Shen, Q.; Krisak, R.; Hagen, K. *J. Mol. Struct.* **1995**, *346*, 13.

(12) Romano, R. M.; Della Védova, C. O.; Downs, A. J. *J. Phys. Chem. A* **2004**, *108*, 7179.

(13) de Fonseca, P. T.; Pacheco, J. G.; Samogin, E.; de Castro, A. R. B. *Rev. Sci. Instrum.* **1992**, *63*, 1256.

(14) Naves de Brito, A.; Feifel, R.; Mocellin, A.; Machado, A. B.; Sundin, S.; Hjelte, I.; Sorensen, S. L.; Bjorneholm, O. *Chem. Phys. Lett.* **1999**, *309*, 377.

(15) Cavasso Filho, R. L.; Homem, M. G. P.; Landers, R.; Naves de Brito, A. *J. Electron Spectrosc. Relat. Phenom.* **2005**, *144−147*, 1125.

(16) Cavasso Filho, R. L.; Lago, A. F.; Homem, M. G. P.; Pilling, S.; Naves de Brito, A. *J. Electron Spectrosc. Relat. Phenom.* **2007**, *156−158*, 168.

(17) Cavasso Filho, R. L.; Homem, M. G. P.; Fonseca, P. T.; Naves de Brito, A. *Rev. Sci. Instrum.* **2007**, *78*, 115104.

(18) Zeng, X. Q.; Ge, M.; Sun, Z.; Bian, J.; Wang, D. *J. Mol. Struct.* **2007**, *840*, 59.

(19) Zeng, X. Q.; Yao, L.; Wang, W. G.; Liu, F. Y.; Sun, Q.; Ge, M.; Sun, Z.; Zhang, J. P.; Wang, D. X. *Spectrochim. Acta, Part A* **2006**, *64*, 949.

(20) Yao, L.; Zeng, X. Q.; Ge, M.; Wang, W. G.; Sun, Z.; Du, L.; Wang, D. X. *Eur. J. Inorg. Chem.* **2006**, 2469.

(21) Zeng, X. Q.; Liu, F. Y.; Sun, Q.; Ge, M.; Zhang, J. P.; Ai, X. C.; Meng, L. P.; Zheng, S. J.; Wang, D. X. *Inorg. Chem.* **2004**, *43*, 4799.

(22) Wang, W.; Yao, L.; Zeng, X.; Ge, M.; Sun, Z.; Wang, D.; Ding, Y. *J. Chem. Phys.* **2006**, *125*, 234303.

(23) Li, Y. M.; Zeng, X. Q.; Sun, Q.; Li, H. Y.; Ge, M.; Wang, D. X. *Spectrochim. Acta, Part A* **2007**, *66*, 1261.

(24) Wang, W. G.; Ge, M.; Yao, L.; Zeng, X. Q.; Sun, Z.; Wang, D. X. *ChemPhysChem* **2006**, *7*, 1382.

(25) Cederbaum, L. S.; Domcke, W. *Adv. Chem. Phys.* **1977**, *36*, 205.

(26) Frisch, M. J.; Trucks, G. W.; Schlegel, H. B.; Scuseria, G. E.; Robb, M. A.; Cheeseman, J. R.; Montgomery, J. A., Jr.; Vreven, T.; Kudin, K. N.; Burant, J. C.; Millam, J. M.; Iyengar, S. S.; Tomasi, J.; Barone, V.; Mennucci, B.; Cossi, M.; Scalmani, G.; Rega, N.; Petersson, G. A.; Nakatsuji, H.; Hada, M.; Ehara, M.; Toyota, K.; Fukuda, R.; Hasegawa, J.; Ishida, M.; Nakajima, T.; Honda, Y.; Kitao, O.; Nakai, H.; Klene, M.; Li, X.; Knox, J. E.; Hratchian, H. P.; Cross, J. B.; Adamo, C.; Jaramillo, J.; Gomperts, R.; Stratmann, R. E.; Yazyev, O.; Austin, A. J.; Cammi, R.; Pomelli, C.; Ochterski, J. W.; Ayala, P. Y.; Morokuma, K.; Voth, G. A.; Salvador, P.; Dannenberg, J. J.; Zakrzewski, V. G.; Dapprich, S.; Daniels, A. D.; Strain, M. C.; Farkas, O.; Malick, D. K.; Rabuck, A. D.; Raghavachari, K.; Foresman, J. B.; Ortiz, J. V.; Cui, Q.; Baboul, A. G.; Clifford, S.; Cioslowski, J.; Stefanov, B. B.; Liu, G.; Liashenko, A.; Piskorz, P.; Komaromi, I.; Martin, R. L.; Fox, D. J.; Keith, T.; Al-Laham, M. A.; Peng, C. Y.; Nanayakkara, A.; Challacombe, M.; Gill, P. M. W.; Johnson, B.; Chen, W.; Wong, M. W.; Gonzalez, C.; Pople, J. A. *Gaussian 03*, revision B.04; Gaussian, Inc.: Pittsburgh, PA, 2003.

(27) Nagata, S.; Yamabe, T.; Fukui, K. *J. Phys. Chem.* **1975**, *79*, 2335.

(28) Dugarte, N. Y.; Erben, M. F.; Romano, R. M.; Boese, R.; Yao, L.; Ge, M.; Della Védova, C. O. *J. Phys. Chem. A* **2009**, *113*, 3662.

(29) Nenner, I.; Beswick, J. A. Molecular Photodissociation and Photoionization. In *Handbook on Synchrotron Radiation*; Marr, G. V., Ed.; Elsevier Science/North-Holland: Amsterdam, 1987; Vol. 2, pp 355−462.

(30) Neufeld, D. A.; Wolfire, M. G. *Astrophys. J.* **2009**, *706*, 1594.

(31) Cortés, E.; Erben, M. F.; Geronés, M.; Romano, R. M.; Della Védova, C. O. *J. Phys. Chem. A* **2009**, *113*, 564.

(32) Thaddeus, P.; Guélin, M.; Linke, R. A. *Astrophys. J.* **1981**, *246*, L41.

(33) Stein, S. E. *NIST Chemistry WebBook*; NIST Standard Reference Database No. 69; 2003.http://webbook.nist.gov.

(34) Flammang, R.; Lahem, D.; Nguyen, M. T. *J. Phys. Chem. A* **1997**, *101*, 9818.

(35) Lahem, D.; Flammang, R.; Van Haverbeke, Y.; Nguyen, M. T. *Rapid Commun. Mass Spectrom.* **1997**, *11*, 373.

JP102179W